THE ASTROPHYSICAL JOURNAL, 558:359–368, 2001 September 1

TIMESCALE STRETCH PARAMETERIZATION OF TYPE Ia SUPERNOVA *B*-BAND LIGHT CURVES

G. GOLDHABER,[1,2,3] D. E. GROOM,[2] A. KIM,[2] G. ALDERING,[2] P. ASTIER,[4] A. CONLEY,[2] S. E. DEUSTUA,[2] R. ELLIS,[5,6] S. FABBRO,[4] A. S. FRUCHTER,[7] A. GOOBAR,[8] I. HOOK,[9] M. IRWIN,[5] M. KIM,[2] R. A. KNOP,[2] C. LIDMAN,[10] R. MCMAHON,[5] P. E. NUGENT,[2] R. PAIN,[4] N. PANAGIA,[7] C. R. PENNYPACKER,[2,11] S. PERLMUTTER,[2,3] P. RUIZ-LAPUENTE,[12] B. SCHAEFER,[13,14] N. A. WALTON,[15] AND T. YORK[2]
(THE SUPERNOVA COSMOLOGY PROJECT)
Received 2001 February 6; accepted 2001 May 4

ABSTRACT

R-band intensity measurements along the light curve of Type Ia supernovae (SNe Ia) discovered by the Supernova Cosmology Project (SCP) are fitted in brightness to templates allowing a free parameter the time-axis width factor $w \equiv s(1 + z)$. The data points are then individually aligned in the time axis, normalized, and *K*-corrected back to the rest frame, after which the nearly 1300 normalized intensity measurements are found to lie on a well-determined common rest-frame *B*-band curve, which we call the "composite curve." The same procedure is applied to 18 low-redshift Calán/Tololo SNe with $z < 0.11$; these nearly 300 *B*-band photometry points are found to lie on the composite curve equally well. The SCP search technique produces several measurements before maximum light for each supernova. We demonstrate that the linear stretch factor, *s*, which parameterizes the light-curve timescale, appears independent of *z*, and applies equally well to the declining and rising parts of the light curve. In fact, the *B*-band template that best fits this composite curve fits the individual supernova photometry data when stretched by a factor *s* with $\chi^2/\mathrm{dof} \approx 1$—thus, as well as any parameterization can, given the current data sets. The measurement of the date of explosion, however, is model dependent and not tightly constrained by the current data. We also demonstrate the $1 + z$ light-curve time-axis broadening expected from cosmological expansion. This argues strongly against alternative explanations, such as tired light, for the redshift of distant objects.

Subject headings: cosmological parameters — galaxies: high-redshift — supernovae: general

1. INTRODUCTION

In systematic searches over the last 12 yr the Supernova Cosmology Project (SCP) has discovered and studied over 100 supernovae, most of which have been spectroscopically identified as Type Ia supernovae (SNe Ia) at redshifts up to $z = 1.20$. Forty-two of these events have so far been used for measurements of the cosmological parameters Ω_M and Ω_Λ (Perlmutter et al. 1999, hereafter P99; see also Perlmutter et al. 1997a presented at a conference in Aigua Blava (Spain) in 1995, and Perlmutter et al. 1997b, hereafter P97a and P97b, respectively). See also Riess et al. (1998), who used 16 high-redshift SNe in a parallel study of the cosmological parameters. An important element of these studies has been the recognition of homogeneity within a one-parameter family of SN Ia light curves.

Several approaches have been used to characterize the SN Ia light-curve family. Phillips (1993) first suggested that the range of SNe Ia light curves might be grouped into a single family of curves parameterized by their initial rate of decline (see also the earlier suggestions of Pskovskii 1977, 1984). Phillips (1993) and Hamuy et al. (1995) further observed that the absolute magnitudes of SNe Ia at maximum light were tightly correlated with this decline rate in the *B*-band light curve—brighter SNe Ia have wider light curves that decline more slowly.Riess, Press, & Kirshner (1995, 1996) introduced an alternative characterization of this range of light curves, in which a scaled "correction template" is added or subtracted from a standard template, effectively widening or narrowing the shoulders of the light curve and thus varying its timescale. In our analyses (P97a, P97b, P99) we instead parameterized the timescale of the SN Ia light curve by a simple "stretch factor," *s*, which linearly stretches or contracts the time axis of a template light curve around the date of maximum light, and thus affects both the rising and declining part of the light curve for each supernova. All three methods of characterizing the light-curve shape or timescale have been used to calibrate the peak magnitudes.

In this paper, we use the data set of supernovae studied in P99 to examine the empirical behavior of SN Ia light curves, and show that this single parameter, the stretch factor *s*, can effectively describe almost all the diverse range of *B*-band light curve shapes over the peak weeks. The stretch-factor method was originally introduced and tested (P97a) without the benefit of either detailed or early data.

[1] gerson@lbl.gov.
[2] E. O. Lawrence Berkeley National Laboratory, Berkeley, CA 94720.
[3] Center for Particle Astrophysics, University of California, Berkeley, CA 94720.
[4] Laboratoire de Physique Nucléaire des Hautes Énergies, CNRS-IN2P3, University of Paris VI & VII, Paris, France.
[5] Institute of Astronomy, Cambridge University, Madingley Road, Cambridge CB3 0HA, UK.
[6] Current address: California Institute of Technology, Pasadena, California.
[7] Space Telescope Science Institute, 3700 San Martin Drive, Baltimore, MD 21218.
[8] Fysikum, University of Stockholm, S-11385 Stockholm, Sweden.
[9] Institute for Astronomy, The University of Edinburgh, Edinburgh EH9 3HJ, Scotland.
[10] European Southern Observatory, La Silla Observatory, Av. El Santo 1538, La Serena, Chile.
[11] Also Space Sciences Laboratory, MC 7450, University of California, Berkeley, CA 94720.
[12] Department of Astronomy, University of Barcelona, Av. Diagonal, 647, E-08028 Barcelona, Spain.
[13] Department of Astronomy, Yale University, P.O. Box 208101, New Haven, CT 06520-8101.
[14] Current address: University of Texas, Austin, TX.
[15] Isaac Newton Group, La Palma, Spain.

We can now test whether it applies to the entire curve, rather than just to the postmaximum decline, and determine the scatter about this scaled curve.

This paper is organized as follows. In § 2 we present the set of supernova and the data used in this analysis. In § 3 we use fits to a preexisting template light curve to cross-compare our data from each supernova and to produce a single composite plot of all the data together. We use the data set of the composite plot to test the validity of our light-curve model and of the stretch parameter. In § 4, we test the hypothesis that redshift is due to cosmological expansion by studying the predicted $(1 + z)$ broadening of the light curves, and we look for evidence for possible supernova evolution. Finally, in § 5 we present a general discussion.

2. DATA

A paper based on our first seven SNe gives the details of our photometric and spectroscopic measurements, as well as the analysis methods (P97b; see also P99). Most of the objects were followed photometrically for over a year. Except for a few SNe discovered before 1995, most spectra were obtained at an early enough epoch at the Keck 10 m telescopes to observe both the characteristic Type Ia SN spectrum and the host galaxy spectrum. Redshifts were determined primarily from narrow emission and absorption lines in the host galaxy spectra. In this paper we are mainly concerned with 35 of the 42 fully analyzed SNe reported in P99 that are listed in Table 1. The redshifts for this 35 supernova subset, $0.30 \leq z \leq 0.70$, are such that "cross-filter K-corrections" are made from the observed Kron-Cousins R to the rest-frame B band (Kim, Goobar, & Perlmutter 1996; Nugent, Kim, & Perlmutter 2001), for which lower redshift data are available for comparison. Of the 42 SNe, seven are omitted here: two $z < 0.3$ and three $z > 0.7$ supernovae, which must be K-corrected to the V and U bands, respectively, are not included here. One distinctly faint outlier, SN 1997O, about 1.5 mag fainter than the average, is also omitted. We have checked that it makes no significant difference whether this SN is included or not. SN 1994G is omitted because of sparse and late R photometry; it was observed primarily in the I-band. We consider one of the supernovae included in this study, SN 1994H, to be unlikely to be Type Ia, based on our more recent analyses (P99; Nugent et al. 2001). It was included here for cross-comparison with the analyses of P97b and P99 (in which it was excluded from the primary analyses); we have checked that its light curve mimics a Type Ia SN quite well, and that including it in this study makes no significant difference. The lower redshift sample used here consists of 18 SNe selected from the 29 SNe of the Calán/Tololo set (Hamuy et al. 1995, 1996), based on the criterion that they were discovered prior to 5 days after maximum light. This homogeneous sample is chosen since it is the low-redshift sample used in P99, which required SNe in the Hubble flow (beyond $z \approx 0.02$) for comparison with the high-redshift sample. We have also examined an additional set of 18 SNe that satisfy the criterion of discovery prior to 5 days after maximum, as discussed below.

The SCP search strategy (P97a) ensures early points by obtaining a set of several baseline "reference images" a few days after new moon, and another set of several "search images" about 3 weeks later. This ensures almost 2 weeks of dark time after discovery for spectroscopic and photometric follow-up. Supernova candidates are found by differencing the pairs of images. The supernova may or may not be present, but in any case is much fainter on the reference set; this is established from archival references or references obtained a year later. The procedure yields one, or even two, image sets for most SNe on the early rising light curve.

TABLE 1

FIT PARAMETERS FOR 42 TYPE 1a SUPERNOVAE REPORTED BY THE SUPERNOVA COSMOLOGY PROJECT (PERLMUTTER ET AL. 1999)

SN Name	z	w	σ_w	s	σ_s	χ^2/dof	Comments
1992bi	0.458	2.26	0.34	1.55	0.23	0.91	
1994F	0.354	0.96	0.19	0.71	0.14	1.74	
1994G	0.425	1.32	0.24	0.92	0.17	0.71	late[a]
1994H	0.374	1.19	0.07	0.87	0.05	1.59	
1994al	0.420	1.22	0.13	0.86	0.09	0.94	
1994am	0.372	1.22	0.05	0.89	0.04	1.73	
1994an	0.378	1.44	0.23	1.04	0.17	1.38	
1995aq	0.453	1.27	0.15	0.87	0.10	1.21	
1995ar	0.465	1.42	0.21	0.97	0.14	2.06	
1995as	0.498	1.64	0.16	1.09	0.11	0.57	
1995at	0.655	1.84	0.12	1.11	0.07	0.80	
1995aw	0.400	1.62	0.06	1.16	0.04	1.80	
1995ax	0.615	1.88	0.18	1.16	0.11	1.17	
1995ay	0.480	1.36	0.12	0.92	0.08	1.07	
1995az	0.450	1.41	0.10	0.97	0.07	0.63	
1995ba	0.388	1.36	0.06	0.98	0.04	1.13	
1996cf	0.570	1.61	0.11	1.03	0.07	1.06	
1996cg	0.490	1.58	0.07	1.06	0.05	0.85	
1996ci	0.495	1.53	0.07	1.02	0.05	1.21	
1996ck	0.656	1.51	0.20	0.91	0.12	1.06	
1996cl	0.828	2.07	0.53	1.13	0.29	1.12	U band
1996cm	0.450	1.33	0.09	0.92	0.06	0.80	
1996cn	0.430	1.28	0.10	0.89	0.07	1.30	
1997F	0.580	1.62	0.11	1.02	0.07	0.86	
1997G	0.763	1.71	0.30	0.97	0.17	1.17	U band
1997H	0.526	1.38	0.08	0.90	0.05	0.86	
1997I	0.172	1.11	0.04	0.94	0.03	5.60[b]	V band
1997J	0.619	1.63	0.21	1.00	0.13	0.94	
1997K	0.592	1.87	0.30	1.18	0.19	0.62	
1997L	0.550	1.51	0.14	0.98	0.09	2.57	
1997N	0.180	1.21	0.02	1.03	0.02	1.72	V band
1997O	0.374	1.40	0.10	1.02	0.07	0.75	outlier
1997P	0.472	1.40	0.06	0.95	0.04	1.30	
1997Q	0.430	1.36	0.04	0.95	0.03	1.09	
1997R	0.657	1.65	0.12	0.99	0.07	1.06	
1997S	0.612	1.90	0.10	1.18	0.06	1.66	
1997ac	0.320	1.39	0.03	1.05	0.02	0.79	
1997af	0.579	1.39	0.08	0.88	0.05	0.95	
1997ai	0.450	1.52	0.20	1.04	0.14	0.82	
1997aj	0.581	1.49	0.09	0.94	0.06	1.75	
1997am	0.416	1.55	0.07	1.10	0.05	1.24	
1997ap	0.830	1.88	0.09	1.03	0.05	1.04	U band

NOTE.—For the present analysis we require good R-band photometry and K-corrections to B, so the seven objects with qualifying comments are not used.

[a] No R-band data before 14 days; primary photometry from I band.

[b] Here the V template was used, while a template between V and R would be more appropriate. A fit to Parab-18 gives χ^2/dof = 2.8.

3. REDUCTION TO A STANDARD B-BAND LIGHT CURVE

In the data analysis as described in P97b and P99, each SN's flux light-curve points are fitted to an R-band template light curve using the nonlinear fitting program MINUIT (James & Roos 1994). For R-band photometric data, the

function

$$\frac{I(t)}{I_{\max}} = f_R\left(\frac{t - t_{\max}}{s(1+z)}\right) + b \qquad (1)$$

is fitted to the data by adjusting the intensity $I_{\max}$ at maximum light, the time of maximum $t_{\max}$, and the stretch factor s so that the width factor $w \equiv s(1+z)$ scales the template time axis, and a baseline level b whose amplitude is found to be <0.02 and allows for small corrections in the background galaxy subtraction.

The function f_R is generated from a *B*-band template (in magnitude) $[F_B(t)]$ *K*-corrected to the *R* band for the given redshift, z, converted to flux and renormalized to unity at light maximum: $f_R(0) = 1$. We use as a template "SCP1997," the same used in P97b and P99 and given in flux in Table 2 (Leibundgut 1988. SPC1997 was based on empirical fits by Leibundgut (shown in col. [2] of Table 2 in flux), tabulated for $-5 \le t \le 110$ days (Leibundgut 1988; see also Leibundgut et al. 1991), and then extended by us with updated data to both late and early times. The constant slope in magnitude, $dm_B/dt = 0.0166$ day^{-1} for days 50–110 was extrapolated to even later times. A piecewise quadratic curve was adjusted to give a reasonable fit to the data for eight nearby Type Ia SNe[16] for $-15 \le t \le -5$ days, and the slope defined by the two earliest points in magnitude (-0.5041 day^{-1}) was extrapolated to earlier times. This linear extrapolation in

[16] SN 1990N, SN 1990af, SN 1991T, SN 1992A, SN 1992bc, SN 1992bo, SN 1994D, and SN 1994ae.

TABLE 2

B TEMPLATES, IN NORMALIZED FLUX, USED BY THE SUPERNOVA COSMOLOGY PROJECT

Day	SCP1997	Parab-18	Parab-20	Day	SCP1997	Parab-18 and -20
-25.....	0.001	0.000	0.000	13.....	0.449	0.466
-24.....	0.001	0.000	0.000	14.....	0.404	0.423
-23.....	0.002	0.000	0.000	15.....	0.363	0.381
-22.....	0.003	0.000	0.000	16.....	0.327	0.342
-21.....	0.005	0.000	0.000	17.....	0.293	0.306
-20.....	0.007	0.000	0.000	18.....	0.264	0.272
-19.....	0.012	0.000	0.005	19.....	0.238	0.241
-18.....	0.019	0.000	0.019	20.....	0.215	0.215
-17.....	0.030	0.005	0.044	21.....	0.195	0.192
-16.....	0.048	0.025	0.080	22.....	0.178	0.172
-15.....	0.076	0.063	0.127	23.....	0.162	0.155
-14.....	0.120	0.118	0.183	24.....	0.149	0.142
-13.....	0.189	0.190	0.248	25.....	0.137	0.130
-12.....	0.277	0.279	0.324	26.....	0.127	0.120
-11.....	0.388	0.385	0.410	27.....	0.118	0.112
-10.....	0.494	0.508	0.508	28.....	0.110	0.105
Day	SCP1997	Parab-18 and -20		29.....	0.103	0.099
-9	0.597	0.622		30.....	0.097	0.094
-8	0.674	0.714		31.....	0.092	0.090
-7	0.746	0.789		32.....	0.087	0.087
-6	0.810	0.849		33.....	0.083	0.084
-5	0.868	0.896		34.....	0.080	0.081
-4	0.915	0.933		35.....	0.076	0.078
-3	0.952	0.961		36.....	0.074	0.076
-2	0.979	0.982		37.....	0.071	0.073
-1	0.995	0.995		38.....	0.069	0.071
0	1.000	1.000		39.....	0.067	0.069
1	0.995	0.995		40.....	0.065	0.067
2	0.979	0.978		41.....	0.064	0.065
3	0.953	0.950		42.....	0.062	0.064
4	0.918	0.910		43.....	0.061	0.062
5	0.875	0.863		44.....	0.060	0.060
6	0.827	0.811		45.....	0.059	0.059
7	0.773	0.759		46.....	0.058	0.058
8	0.718	0.707		47.....	0.057	0.057
9	0.661	0.656		48.....	0.056	0.056
10	0.604	0.606		49.....	0.055	0.055
11	0.550	0.558		50.....	0.054	0.054
12	0.498	0.511				

NOTE.—SCP1997 refers to Leibundgut 1988 from day -5 on up, with a linear extension (in magnitude) to earlier times shown in flux here. As discussed in the text, this is the template used in Perlmutter et al. 1997, 1999. Tables 1, 3, and 7 as well as Fig. 2*e*, are based on this template. Parab-18 uses a parabolic turn-on at -17.6 days from a fit to the 35 SCP SNe. Tables 4 and 7 and Figs. 1 and 2, except 2*c* and 2*e*, are based on this template. Parab-20 uses the parabolic turn-on at -20 days following the early rise-time data of Riess et al. 1999b. Table 5 and Fig. 2*c* are based on this template. After -10 days, the two parabolic templates coincide.

magnitude is exponential in flux. Only a handful of measurements were available for $t < -10$ days, and the earliest behavior rested on single measurements of SN 1994ae at -12.9 days and SN 1994D at -14.8 days in the observer system. This template was used for our cosmology analysis (P97b; P99). Note that since all fits to data were performed starting with this template, this template has a stretch factor of $s = 1$ by definition.

The results of the fits are shown in Table 1, which gives the redshift, z, the measured width factor, w, in the observer system and the corresponding stretch factor, s, as well as the measurement errors, σ_w and σ_s, and the χ^2/dof for the MINUIT fits. Table 3 gives the same information for the Calán/Tololo low-redshift data.

The systematic uncertainty in the time-dependent K-corrections, recalculated for P99, are estimated as <0.02 mag for the light-curve phases later than $\simeq -14$ days. An effect we need to consider in determining the early-time light-curve behavior is how uncertainties in the K-corrections at these early epochs propagate into uncertainties on the K-corrected B-band fluxes. In particular, we need to examine all the points that occur prior to day -14 with respect to maximum light. Later than this epoch we have the necessary spectroscopy of a variety of SNe Ia to perform accurate K-corrections. Prior to this we have tied all the K-corrections to our knowledge of the spectral energy distribution (SED) of SNe Ia at this earliest epoch.

At a redshift of $z \approx 0.5$, the uncertainty in the K-corrections as a function of epoch is negligible because of the nice alignment of the B- and R-band filters (Kim et al. 1996). For SNe Ia at redshifts below this value (to $z = 0.3$, our nominal cutoff for SN Ia included in this study) the B to R K-correction (K_{BR}) involves knowledge of the SED redward of the B-band filter. For SNe Ia beyond this redshift (to $z = 0.7$, our other cutoff) K_{BR} relies on our understanding of the U-band behavior of SNe Ia. For a simple and very conservative test, we can gain an understanding of the uncertainties by looking at the K-corrections at these two extreme redshifts, which involve the greatest extrapolation and hence would produce the largest error.

For $z = 0.3$ and day -14, we find $K_{BR} = 0.51$ for a SN Ia from a spectral analysis. This value corresponds to the value that a $\approx 15{,}000$ K blackbody would give at this redshift. From the models of Höflich (1995), Nugent et al. (1997), and Lentz et al. (2000), we can see that in the optical spectra redward of 4000 Å, at the earliest epochs after explosion, SNe Ia closely approximate blackbodies with a very minimal contribution from the lines ($<10\%$) to the overall SED. The exact temperature is not critical in going from 15,000 to 100,000 K. Using a 100,000 K blackbody as a model of the earliest epoch for a SN Ia (a gross overestimate of its temperature, since the γ-rays from the decay of ^{56}Ni have not had enough time to propagate out and heat up the atmosphere), K_{BR} only changes by 0.07 mag. This is well below the difference that can be distinguished by the data sets at these very early epochs. Only one SN Ia above a redshift of 0.6 (where the K-corrections start to involve a decent amount of extrapolation), SN 1995at, contributes to the early light curve prior to day -14. SN 1995at was observed at day -16.3 and was at $z = 0.655$. The effect of this single photometry point on our calculations is negligible. In addition, all of the models mentioned above show very little difference in the overall SED over the epochs -14 to -16.3 days.

TABLE 3

Fit Parameters for the Calán/Tololo Data

SN Name	z	w	σ_w	s	σ_s	χ^2/dof
1990O	0.030	1.09	0.03	1.06	0.03	1.53
1990af	0.050	0.82	0.02	0.78	0.02	0.51
1992P	0.026	1.15	0.08	1.12	0.08	1.45
1992ae	0.075	1.09	0.09	1.02	0.08	0.78
1992ag	0.026	1.14	0.04	1.11	0.04	2.15
1992al	0.014	0.99	0.02	0.98	0.02	1.71
1992aq	0.101	1.04	0.14	0.95	0.13	0.65
1992bc	0.020	1.12	0.01	1.09	0.01	3.14
1992bg	0.036	1.09	0.05	1.05	0.05	1.68
1992bh	0.045	1.15	0.05	1.10	0.05	3.77
1992bl	0.043	0.92	0.03	0.88	0.03	2.15
1992bo	0.018	0.77	0.01	0.76	0.01	1.29
1992bp	0.079	1.03	0.03	0.95	0.03	1.35
1992br	0.088	0.58	0.04	0.53	0.04	1.39
1992bs	0.063	1.05	0.05	0.99	0.05	1.43
1993B	0.071	1.06	0.09	0.99	0.08	1.14
1993O	0.052	0.99	0.01	0.94	0.01	1.26
1993ag	0.050	1.01	0.04	0.96	0.04	1.16

3.1. *A Composite Light Curve*

We now introduce the concept of a "composite light curve," constructed by linearly compressing or expanding the time axis for each SN such that all the low- and high-z data points can be plotted on a single curve. To study the light-curve data in this composite form, a further step is added to the procedure of P97b and P99: after the time of maximum, $t_{\max}$, and the stretch factor for each SN is obtained from the fit, the individual R-band data points are K-corrected back to points in the equivalent rest-frame B band.

Figure 1 presents all photometry points in composite light curves for the template "Parab-18," which is an improved template over SCP1997, as discussed below. The left-hand figures 1*a*, 1*c*, and 1*e* show a data point for each night's observation of each supernova, whereas the right-hand Figures 1*b*, 1*d*, and 1*f* show 1 day averages over all supernovae. The K-corrected SCP points for SNe with $0.30 \leq z \leq 0.70$ are shown as solid red circles. Shown as blue squares are K-corrected points (K_{BB}) for the 18 SNe from the Calán/Tololo study in the B-band (Hamuy et al. 1996) with $z < 0.11$. Figures 1*a* and 1*b* show the B-band photometry points in the observer system displaced to $t = 0$ at light maximum, and normalized to unit intensity at $t = 0$. There are no corrections for stretch or width; times of observation relative to maximum light are used. In Figures 1*c* and 1*d* we have transformed the time axis from the observer frame to the rest frame by dividing by the appropriate $1 + z$ for each data point of each of the SNe. Finally, in Figures 1*e* and 1*f*, for each supernova we also divide the timescale for each point by the fitted stretch factor s. By this stage essentially all of the dispersion has been removed, and the corrected points for both the SCP and Calán/Tololo data fall on a common curve at the level of the measurement uncertainty, of typically 2%–4%. It is remarkable that application of this single stretch timescale parameter results in such a homogeneous composite curve.

3.2. *The Templates*

While we used the exponential rise in our fits to s, $t_{\max}$, $I_{\max}$, and b with the SCP1997 light-curve template, in reality

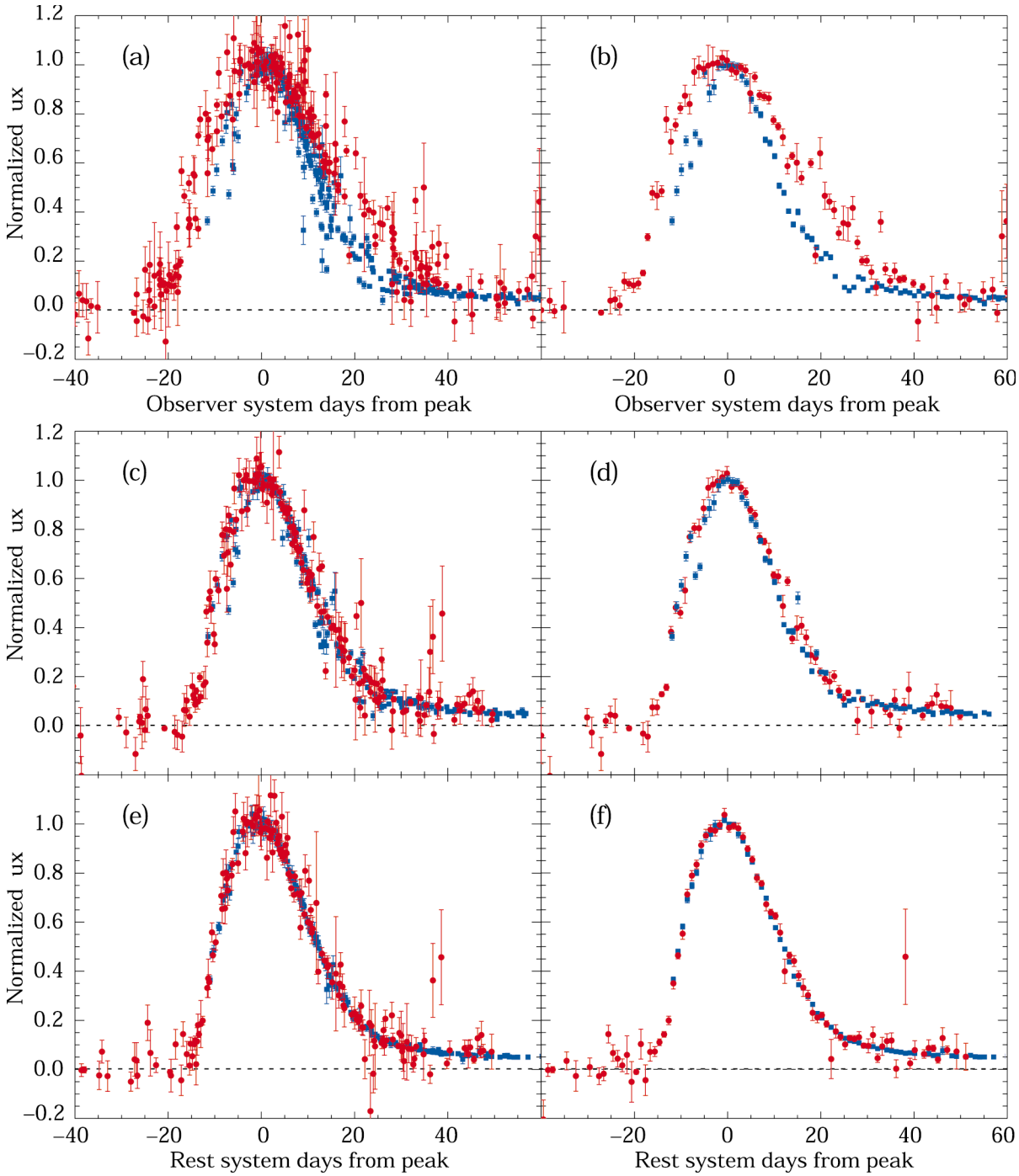

FIG. 1.—(*a*) Photometry points for the 35 SCP (*filled red circles*) and 18 Calán/Tololo SNe (*blue squares*), fitted to Parab-18 with the maximum flux normalized to unity and the time of maximum adjusted to zero in the observer system. (*b*) The same data averaged over 1 day intervals and over each set of SNe. (*c*)–(*d*) The same data transformed to the rest system. In (*e*) and (*f*), the time axis for each photometry point is additionally divided by the corresponding stretch factor *s*.

there must be a definite explosion date, $t_{\rm exp}$. To find an improved early template for the composite light curve, we use a parabolic approximation to the initial light curve and determine its two parameters, the explosion date $t_{\rm exp}$ and timescale parameter a, by calculating a least-squares fit of the function $I(t)/I(0) = a(t - t_{\rm exp})^2$ to the UN-averaged stretch-corrected composite flux data (which, unlike magnitudes, have Gaussian errors). (Since the fits were to the stretch-corrected composite data, the actual explosion day of any individual supernova is $t_0 = st_{\rm exp}$.) We determined that fitting the early-time parabola to the later-time exponential template (matching both the value and first derivative) was not very sensitive to the join date in the epoch around -10 days.

Using this additional form for the early part of the light curve, we can compare the combined composite light curve of Figure 1*f* with three forms of the template $F_B(t)$:

1. *The SCP1997 template.*—This light-curve template (listed in Table 2) begins with a linear rise in magnitude

(exponential in flux); it was used in P97b and P99. The width factor and stretch factor values given in Tables 1 and 3 come from fits to this template and are supplementary to Tables 1 and 3 in P99.

2. *The "Parab-18" template.*—This light-curve template (listed in Table 2) begins with a parabolic rise in flux; its explosion date at −17.6 days is based on a parabolic fit to the composite data (starting from the SCP1997 template). A cubic spline fit to the data beyond the "join date" at −10 days improves the template fit as compared to SCP1997 (or Leibundgut), in particular near −5 days. This template thus gives the best fit to the SCP data, although the fit to Parab-20 (see next item) is nearly as good. Whenever so stated the analyses in this paper are based on this template.

3. *The "Parab-20" template.*—This light-curve template (listed in Table 2) also begins with a parabolic rise in flux, but with an explosion date at −20.0 days based on the recent early data of Riess et al. (1999b). At later times, after day −10, it is the same as Parab-18, and thus differs by only a small amount from the SCP1997 template. This template also gives an acceptable fit to the composite data, as also found by Aldering, Knop, & Nugent (2000; hereafter AKN00).

Figure 2*a*, based on Parab-18, shows that this template accounts well for all the data points in our composite sample. Both the SCP and the Calán/Tololo data scatter about this template with a dispersion that is expected from their measurement uncertainties. From the residual plots of Figures 2*b* and 2*d*, it is clear that this day-by-day uncertainty is less than 2%–4% (0.02–0.04 mag) for almost the entire period from day −10 to day 40. The χ^2 distributions for the residuals are given in Table 4 (Parab-18) for the 35 SCP SNe in 5 day intervals from −25 to 40 days and, in the last line, for this entire interval.

A good fit to the data is also obtained for Parab-20, corresponding to $t_{exp} = -20$ days, for which we give the residual plot in Figure 2*d* and the χ^2 distributions for the residuals in Table 5. Fitting the data to this new template, Parab-20, results in the fitting program MINUIT slightly readjusting the stretch s, intensity at maximum light I_{max}, and the time of maximum t_{max} for each SN. The average change in m_B^{eff} from the values found using the SCP1997 template, for the 35 SCP SNe, is −0.005. The corresponding average change in m_B^{eff} for the 18 Calán/Tololo SNe is −0.014. Thus, the net change in difference between low- and high-redshift m_B^{eff} is 0.009. This is the only quantity that enters into the cosmological measurements via the distance modulus. The rising part of the curve for both templates Parab-18 and Parab-20 fits our data equally well, with only a negligible change in the overall χ^2/dof from 0.905 to 0.906 for the epoch −25 to 40 days. Either of the above templates

TABLE 4

χ^2 FITS OF THE SCP DATA TO THE COMPOSITE PARABOLIC TEMPLATE PARAB-18 CORRESPONDING TO $t_{exp} = -17.6$ DAYS

EPOCH			
Start (1)	End (2)	χ^2 (3)	χ^2/dof (4)
−25	−20	27.8	1.16
−20	−15	23.7	0.99
−15	−10	35.8	0.58
−10	−5	72.4	0.95
−5	0	101.7	1.02
0	5	111.6	0.88
5	10	74.5	0.89
10	15	62.2	0.91
15	20	25.6	0.47
20	25	83.3	0.95
25	30	70.1	1.02
30	35	49.1	0.88
35	40	25.8	1.51
−25	40	763.5	0.905

NOTE.—Cols. (1) and (2) define the epoch interval, cols. (3) and (4) give the χ^2 and χ^2 per degree of freedom. See Fig. 2*b*.

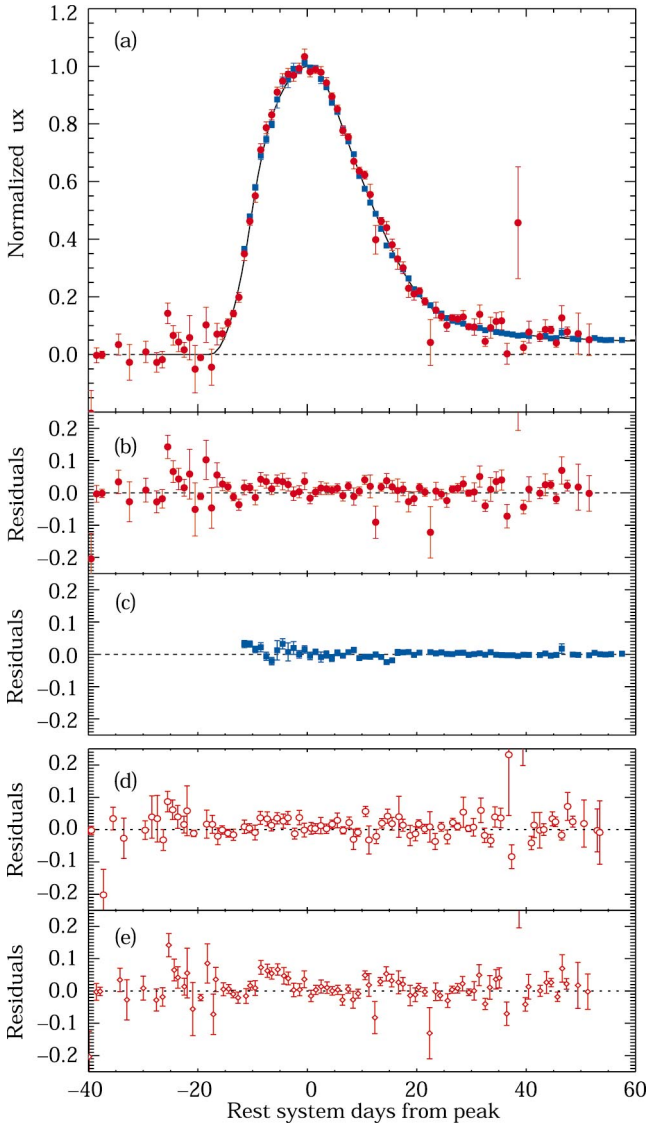

FIG. 2.—(*a*) Same distribution as in Fig. 1*f*, with the SNe in the two data sets fitted to Parab-18. The template curve for Parab-18 is shown in black. (*b*) Residuals for the SCP (*filled red circles*) photometry fits to Parab-18. Here the epoch between -40 and -20 days has no SN signal; the data come from the reference images, which have shorter exposures and hence larger errors (see Table 4). (*c*) Residuals for the Calán/Tololo (*blue squares*) photometry fits to Parab-18 (see Table 7). (*d*) Open red circles show the residuals for the SCP data from the fit to Parab-20 (template not shown), where the early rise is based on the data of Riess et al. (1999b); see Table 5. (*e*) Residuals for the SCP data (*open red diamonds*) fitted to the template SCP1997 (template not shown). Note that the "bumps" near −5 and 15 days (see also Table 6) were eliminated for the templates Parab-18 and Parab-20.

TABLE 5

χ^2 FITS OF THE SCP DATA TO THE COMPOSITE PARABOLIC TEMPLATE PARAB-20 CORRESPONDING TO $t_{exp} = -20$ DAYS

EPOCH			
Start (1)	End (2)	χ^2 (3)	χ^2/dof (4)
−25	−20	29.3	1.01
−20	−15	27.5	0.65
−15	−10	28.4	0.71
−10	−5	71.2	0.94
−5	0	105.0	1.00
0	5	115.6	0.92
5	10	70.1	0.86
10	15	63.6	0.96
15	20	26.1	0.49
20	25	84.6	0.95
25	30	67.9	1.03
30	35	52.0	0.91
35	40	21.4	1.34
−25	40	762.6	0.906

NOTE.—Cols. (1) and (2) define the epoch interval, cols. (3) and (4) give the χ^2 and χ^2 per degree of freedom. See Fig. 2*d*

are an improvement over SCP1997, for which we obtain χ^2/dof = 0.966 (see Table 6). However, within the accuracy of our data, any of the three templates is perfectly acceptable.[17] Note that the composite light curve depends in fine detail on the template used to fit and then match the peak and stretch of each individual SN's light curve.

For the Parab-18 template we found $a = 0.0085 \pm 0.0010$ and $t_{exp} = -17.6 \pm 0.5$ days; a preliminary value of -17.5 ± 0.4 was presented in the conference reports of Groom (1998) and Goldhaber (1998a, 1998b). However, it is important to recognize that these uncertainties reflected only the error in mapping the fixed composite light curve to a parabola after fitting with an assumed template (and thus did not include errors that depend on the shape of the early portion of the template used). Since the fits are sensitive to the early portion of the light curve, the total uncertainty on t_{exp} is much larger.

TABLE 6

χ^2 FITS OF THE SCP DATA TO THE COMPOSITE EXPONENTIAL TEMPLATE SCP1997, THE EXTENDED LEIBUNDGUT TEMPLATE

EPOCH			
Start (1)	End (2)	χ^2 (3)	χ^2/dof (4)
−25	−20	27.5	1.15
−20	−15	24.3	1.01
−15	−10	36.8	0.59
−10	−5	105.2	1.38
−5	0	105.7	1.06
0	5	110.8	0.87
5	10	75.3	0.90
10	15	73.4	1.08
15	20	29.3	0.54
20	25	83.8	0.95
25	30	69.1	1.00
30	35	49.2	0.88
35	40	25.4	1.49
−25	40	815.7	0.966

NOTE.—Cols. (1) and (2) define the epoch interval, cols. (3) and (4) give the χ^2 and χ^2 per degree of freedom. See Fig. 2*e*.

[17] Given the low-redshift data presented by Riess et al. (1999b), we believe that the Parab-20 template is likely to be the best current estimate for a single common stretch-parameterized light curve.

TABLE 7

χ^2 FITS OF THE CALÁN/TOLOLO DATA TO THE COMPOSITE PARABOLIC TEMPLATE

EPOCH			
Start	End	χ^2	χ^2/dof
−10	−5	25.3	1.95
−5	0	39.7	2.09
0	5	17.1	0.47
5	10	59.5	1.06
10	15	55.7	1.39
15	20	28.9	1.25
20	25	14.8	0.93
25	30	11.2	0.62
30	35	21.1	1.32
35	40	17.0	0.81
−10	40	290.3	1.143

NOTE.—In this table some of the photometry errors were extremely small. We used a minimum error of 0.007 here, in normalized units. Cols. (1) and (2) define the epoch interval, cols. (3) and (4) give the χ^2 and χ^2 per degree of freedom. See Fig. 2*c*.

For comparison with AKN00, we have analyzed the same more restrictive set of 30 SCP SNe with $0.35 \leq z \leq 0.65$, leaving out SN 1997aj.[18] A simple χ^2 study of these SNe, fitting them to a series of parabolic-rise templates as a function of explosion dates, yields higher statistical uncertainties $t_{exp} = -(17.8^{+1.9}_{-1.0}$ statistical), corresponding to a 1 σ range of −19.7 to −16.8 days. This statistical uncertainty is consistent with the more comprehensive analysis of AKN00, which accounted for the full multidimensional probability distribution as well as upper limits on several systematic uncertainties, and found $t_{exp} = -(18.3^{+1.2}_{-1.2}$ statistical $^{+3.6}_{-1.9}$ systematic) at $t_{join} = -10$ days. Note that the exact shape of the early portion of the light curve does not significantly affect the values or uncertainties of the cosmology results of P99 (see AKN00 as well as our results above).

Only future data will be able to tell whether all Type Ia SNe can be adequately described by *s* only or whether some variation in t_{exp} will also be needed. This will require very early SN detection, corresponding *K*-corrections, and spectra as are envisioned for the *Supernova/Acceleration Probe* (*SNAP*) satellite project, currently under design.[19]

Table 7 gives the corresponding data for the 18 Calán/Tololo SNe from −10 to 40 days. Since there are no significant data before −10 days, Parab-18 and Parab-20 coincide in this case. For these data, the first two epochs

[18] The fits for SN 1997aj undergo a large change in stretch, from 0.94 to 1.52, in going from the template SCP1997 to Parab-20. Because of this feature, this SN was excluded by AKN00 and in the 30 SN sample here. However, in the χ^2 distributions quoted in Tables 4 and 5 all 35 SNe were included.

[19] See http://snap.lbl.gov for information on SNAP.

give a rather high χ^2/dof of ~ 2. We note that at these two epochs the data come primarily from only two SNe; of these only SN 1992bc has a poor overall χ^2 (see Table 3), and in particular is responsible for the high χ^2 values at the two epochs. To improve our understanding of the early epochs we have also studied 18 additional low-redshift SNe, which, however, are not discovered in a homogeneous search and are not all in the Hubble flow. These SNe consist of 16 of the 22 SNe given by Riess et al. (1999a), which fulfill the criterion of being discovered prior to 5 days after maximum light, as well as SN 1990N from Lira et al. (1998) and SN 1998bu from Suntzeff et al. (1999) as extended to earlier times (before -10 days) by Riess et al. (1999b). This low-redshift sample fits the Parab-20 template from -15 to 40 days with a χ^2/dof of 1.015, thus agreeing well with the 18 Calán/Tololo SNe in the overlap region. This study of the second set of 18 SNe will be presented in a future publication.

3.3. *The Universality of the Stretch Factor*

The stretch factor applies to both the rising and the falling part of the light curve. A qualitative impression of this can be obtained from a comparison of Figures 1*c* and 1*e*, as well as 1*d* and 1*f*. To obtain a quantitative result we took two approaches. In Table 8 we show the χ^2 distribution for the case in which only $1 + z$ but not s has been factored out of the observer-frame distribution; this corresponds to Figures 1*c* and 1*d*. Here we note large χ^2 values both before and after maximum light, indicating that ignoring s affects both distributions. Second, we have taken the individual photometry points of the composite curve and split them into two groups at epoch $t = 0$. We then fitted each half with MINUIT to determine a stretch. This gave $s = 1.03 \pm 0.04$ with $\chi^2 = 352$ for 366 dof for the epoch $< t_{\max}$ and $s = 1.00 \pm 0.02$ with $\chi^2 = 894$ for 996 dof for the epoch $> t_{\max}$. The period $> t_{\max}$ encompassed all the photometry points out to over 1 yr. The equality of s, within statistical errors, for the two groups shows that the same value of s applies to both.

TABLE 8

χ^2 Fits of the SCP Data to the Parabolic Template Parab-18 with Only $1 + z$ but Not s Factored Out

Epoch			
Start (1)	End (2)	χ^2 (3)	χ^2/dof (4)
-25.....	-20	24.2	1.86
-20.....	-15	30.3	1.08
-15.....	-10	231.8	4.55
-10.....	-5	250.2	3.05
-5	0	104.3	1.03
0.....	5	112.4	0.89
5.....	10	125.6	1.38
10	15	57.9	0.95
15	20	110.1	1.84
20	25	98.6	1.15
25	30	105.0	1.36
30	35	45.9	1.12
35	40	35.4	1.18
-25.....	40	1330.7	1.582

Note.—This table illustrates the effect of the factor s both before and after maximum light. Cols. (1) and (2) define the epoch interval, cols. (3) and (4) give the χ^2 and χ^2 per degree of freedom.

As can be noted from Tables 4 and 7 as well as Figure 2*b* and 2*c*, the factor s combined with the factor $1 + z$ brings all the 35 SCP SNe and the 18 Calán/Tololo SNe into agreement with a single curve from -25 to over 25 days as well as can possibly be determined with the present data sets. The stretch-factor parameterization appears to work quite well at least out to day 40, although the high-redshift data are less constraining at these late dates, and there is evidence of at least two low-redshift supernova that may vary from the template at these later epochs (see AKN00).

4. TEST OF COSMOLOGICAL LIGHT CURVE BROADENING AND CHECK FOR SN EVOLUTION

These data also produce compelling evidence that the observed explosion of the supernova itself is slowed[20], due to a dilation effect, by the factor $1 + z$. This provides independent evidence for cosmological expansion as the explanation for redshifts. Although this hypothesis has proved to be consistent with observation for over half a century, persistent doubts are still occasionally expressed (e.g. Marič, Moles, & Vigier 1977; Chow 1977; La Violette 1986; Arp 1987; Arp et al. 1990, 1994; Narlikar & Arp 1993). Surprisingly, until recently very few direct tests of this expansion have been performed. A test by Sandage & Perelmutter (1991), who calculated the surface brightness of brightest cluster galaxies over a range of redshifts, showed compelling evidence for expansion but did not reach a definitive conclusion because of possible systematic errors. An argument has also been made that some gamma-ray bursts (GRBs) should be at cosmological distances because of the observation that for the "longer GRBs," the length of the bursts was inversely correlated to the brightness of the GRBs (Piran 1992; Norris et al. 1995). The discovery of GRBs at cosmological distances strengthens this argument (see, e.g., Metzger et al. 1997); however, since the intrinsic length of a given GRB is unknown, this remains a qualitative argument (Lee, Bloom, & Petrosian 2000).

Using supernova light curves to test the cosmological expansion was first suggested by Wilson (1939; see also Rust 1974). Over the last decade it has become clear that Type Ia SNe, found nearby and at cosmological distances, provide superb and precise clocks for such tests. We presented the first clear observation of the $1 + z$ light-curve broadening, based on our first seven high-z Type Ia SNe (Goldhaber et al. 1997), at a conference in Aigua Blava (Spain) in 1995. Leibundgut et al. (1996) later also gave evidence for the effect, using a single high-z supernova. More recently, Riess et al. (1997) showed evidence that the spectral features of Type Ia SNe can be timed sufficiently well to measure the time interval between two spectra taken 10 days apart in the observer system. Applying this method to one supernova gave results consistent with $1 + z$ light-curve broadening at the 96.4% confidence level. With the current data set, we can now demonstrate the light-curve broadening with a larger, statistically significant sample.

Light-curve width factor w and stretch factor s versus $1 + z$ are shown in Figures 3*a* and 3*b*, respectively, for the Calán/Tololo and SCP SNe. We are interested in the possible variation of w and s with z. We test for the z-

[20] The different usages of the term "time dilation" for light-curve broadening are discussed in Weinberg (1972).

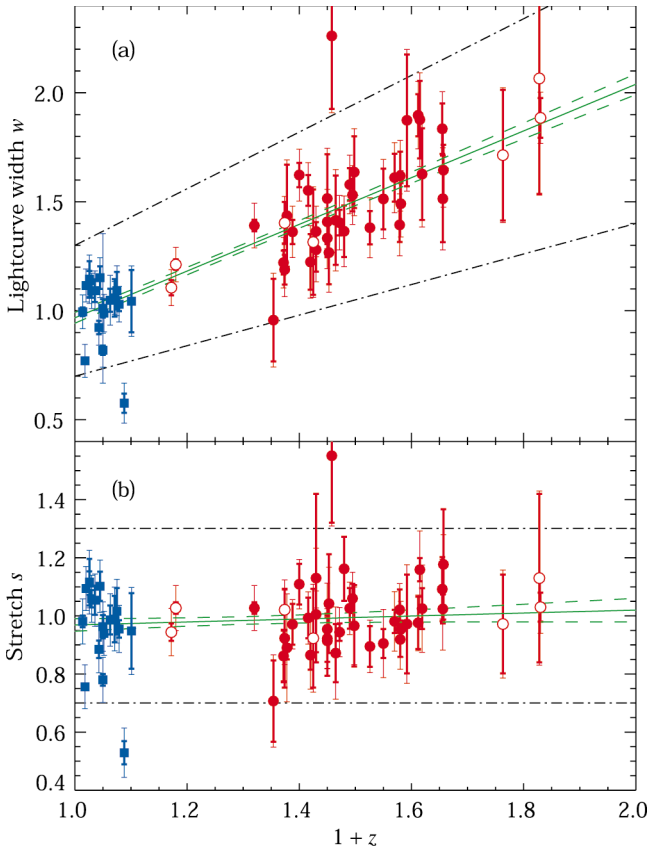

FIG. 3.—(*a*) Observed light-curve width factor w vs. $1 + z$. The blue squares correspond to the Calán/Tololo SNe, and the filled red circles are for the subset of 35 SCP SNe used in this paper. The open red circles are for the remainder of the 42 SCP fully-analyzed SNe. The band delineated by the black dash-dotted lines corresponds to stretch values 0.7–1.3, which encompass the bulk of the data, except for two outliers. The green line shows the best linear fit to the data, as discussed in the text. The band delineated by the two green dashed curves corresponds to the $\pm 1\ \sigma$ values. (*b*) Stretch s vs. $1 + z$. Stretch is defined as the observed light-curve width w divided by $1 + z$ for each SN. The points and lines are defined as in (*a*).

dependence of these distributions by fitting straight lines to the data. If the SNe in the distant past were different, i.e., due to evolution effects, the distribution might show a slope ds/dz. The fits described below were carried out for the entire 17 Calán/Tololo SNe, together with 41 of the SCP SNe. Two SNe, SN 1992bi and SN 1992br, have stretch factors outside the range $0.7 < s < 1.3$, and are excluded from the fits as outliers representing non-Gaussian tails to the distributions or aberrant objects. As discussed in P99, these will not be important for the present analysis.

In performing the fit of the function $s = a + bz$ to the data shown in Figure 3*b*, the total uncertainty for each point is $\sigma_{s'} = (\sigma_s^2 + \delta_s^2)^{1/2}$, where δ_s^2 is the intrinsic stretch dispersion and σ_s from Tables 1 and 3 is from the individual light-curve fit uncertainty. We estimate this intrinsic dispersion by requiring that the reduced χ^2 is near unity. This yields an rms deviation $\delta_s \approx 0.08$. The intrinsic width δ_s of the stretch-factor distribution can also be obtained from a Gaussian fit to Figure 4 in P99. This gives a consistent value for δ_s of ~ 0.1. The errors used in the fit to the w distribution shown in Figure 3*a* are treated similarly. In Figures 3*a* and 3*b* both errors σ_s and $\sigma_{s'}$ are shown on the error bars.

We find that our data is consistent with $1 + z$ light-curve broadening and a redshift-independent SN stretch distribution. Fits to Figures 3*a* and 3*b* yield different information. The linear fit shown in Figure 3*a* has $dw/dz = 1.07 \pm 0.06$. If there were no z-dependence in w this slope would be 0, here assuming no evolutionary change in s. Hence, the evidence for the presence of a $1 + z$ factor is $1.07/0.06 \approx 18$ standard deviations. Figure 3*b* shows a slope $ds/dz = 0.05 \pm 0.05$. The extent by which this slope differs from 0 measures the possible evolution effects on s, here assuming a $1 + z$ dependence of w. The result indicates that $ds/dz < 0.09$ at the 95% confidence level out to $z \sim 0.8$. We obtain essentially the same results from fits in which the two outliers are included (for a total of 60 SNe), and when the 35 rather than the 42 SCP SNe, less two outliers, are used (for a total of 51 SNe). Note that this analysis does not account for sample selection effects (such as possible preferred discovery of high-stretch SNe near the flux limit of each SNe search), which may need to be accounted for in future data sets.

When we compare this result to the alternate theories, it is clear that they are severely challenged or simply ruled out. The tired-light theories (Zwicky 1929; Hubble & Tolman 1935; Hubble 1936; Marič et al. 1977; Chow 1977; La Violette 1986) would not yield this slowing of the light curves, and thus do not fit this data set. Variable-mass theories (Narlikar 1977; Narlikar & Arp 1993, 1997) would apparently require a series of coincidences: the radioactive decay times, the timescales for the radiative transport processes in the SN atmosphere, and the atomic transitions would all have to vary as $(1 + z)$ due to variations in the masses of elementary particles for the theory to account for the data. All these effects would have to result in making the observed spectra similar.

5. DISCUSSION

We have shown that a single stretch factor varying the timescale of the SNe Ia accounts very well for the rest-frame *B*-band light curve both before and after maximum light (up to 40 days past maximum). It is not understood from the current state of the theory of SNe Ia whether this is a fortuitous coincidence or a reflection of some physics timescale (Höflich 1995; Höflich & Khokhlov 1996; Nugent 1997; Pinto & Eastman 2000; Arnett 2000; Hillebrandt & Niemeyer 2000). Although we do not necessarily expect this single-timescale stretch factor to hold for all wavelength bands, we do have evidence that it applies in the *V* band and (with less confidence) the *U* band. We will analyze these results in future work.

The current analysis does not address the relationship between the SN Ia light curve stretch and its peak luminosity. This requires another analysis that will be presented elsewhere. However, it is important to note that the current *B*-band template stretched by a factor s fits the data as well as any parameterization can, given the current data sets. It will therefore yield a peak-luminosity correlation with as small a dispersion as can be obtained by any other *B*-band light-curve parameterization.

The comparison of the low- and high-redshift composite supernovae light curves in Figure 2 provide a first-order test for evolution of supernovae as we go back to the $z \sim 0.5$ epoch. The close match of the light curves suggests that little evolution has occurred.

A recent analysis of low-redshift early light curves by Riess et al. (1999b, 1999c) suggested that the explosion date of the low-redshift SNe Ia was earlier than that of the high-redshift SNe. The analyses of our early light curve uncer-

tainty in § 4 and in AKN00 show that the difference between the two data sets is not very significant at this stage, less than $\sim 2\ \sigma$. This will be an interesting region of the light curve to pursue with future data, particularly over a range of host galaxy environments that would be expected to show variations in metallicity and progenitor ages. We are currently working with the supernova research community on generating a much more extensive low-redshift data set to study this question. However, it is important to remember that (as pointed out by AKN00) the template differences have a negligible influence on the corrected peak magnitudes of the P99 SNe, and thus the cosmological parameters derived therein are unchanged.

Finally, it is interesting to note that while the redshift of the light measures the expansion of the universe with a "microscopic clock" of period, typically $T = 2 \times 10^{-15}$ s, our "macroscopic clocks," the Type Ia SNe, measure the expansion over a ≈ 4 week period, or $T \approx 2.4 \times 10^{6}$ s. The $1 + z$ expansion effect is thus consistent for two time periods that differ by 21 orders of magnitude.

The observations described in this paper were primarily obtained as visiting/guest astronomers at the Cerro Tololo Inter-American Observatory 4 m telescope, operated by the National Optical Astronomy Observatory under contract to the National Science Foundation; the Keck I and II 10 m telescopes of the California Association for Research in Astronomy; the Wisconsin-Indiana-Yale-NOAO (WIYN) telescope; the European Southern Observatory 3.6 m telescope; the Isaac Newton and William Herschel Telescopes, operated by the Royal Greenwich Observatory at the Spanish Observatorio del Roque de los Muchachos of the Instituto de Astrofisica de Canarias; the *Hubble Space Telescope*, and the Nordic Optical 2.5 m telescope. We thank the dedicated staff of these observatories for their excellent assistance in pursuit of this project. In particular, Dianne Harmer, Paul Smith, and Daryl Willmarth were extraordinarily helpful as the WIYN queue observers. We thank Gary Bernstein and Tony Tyson for developing and supporting the Big Throughput Camera at the CTIO 4 m; this wide-field camera was important in the discovery of many of the high-redshift supernovae. This work was supported in part by the Physics Division, E. O. Lawrence Berkeley National Laboratory of the US Department of Energy under contract DE-AC03-76SF000098, and by the National Science Foundation's Center for Particle Astrophysics, University of California, Berkeley under grant ADT 88909616. Support for this work was provided by NASA through grant HST GO-07336 from the Space Telescope Science Institute, which is operated by AURA, Inc., under NASA contract NAS5-26555. A. G. acknowledges the support of the Swedish Natural Science Research Council. The France-Berkeley Fund and the Stockholm-Berkeley Fund provided additional collaboration support.

REFERENCES

Aldering, G., Knop R., & Nugent P. 2000, AJ, 119, 2110
Arnett, W. D. 2000, ApJS, 127, 213
Arp, H. C. 1987, Quasars, Redshifts, and Controversies (Berkeley: Interstellar Media)
Arp, H. C., Burbidge, G., Hoyle, F., Narkikar, J. V., & Wickramasinghe, N. C. 1990, Nature, 346, 807
Arp, H. C., et al. 1994, ApJ, 430, 74
Chow, T. L. 1981, Nuovo Cimento Lett., 32, 351
Goldhaber, G. 1998a, in Proc. 26th Summer Inst. on Particle Physics, Gravity: From the Hubble Length to the Plank Length, ed. D. Burke et al. (Stanford: Stanford Linear Accelerator Center)
———. 1998b, BAAS, 193, 47.13
Goldhaber, G., et al. 1997, in Thermonuclear Supernova, ed. P. Ruiz-Lapuente, R. Canal, & J. Isern (Dordrecht: Kluwer), 777
Groom, D. E. 1998, BAAS, 193, 111.02
Hamuy, M., Phillips, M. M., Maza, J., Suntzeff, N. B., Schommer, R. A., & Aviles, R. 1995, AJ, 109, 1
———. 1996, AJ, 112, 2391
Hillebrandt W., & Niemeyer J. C., 2000, ARA&A, 38, 191
Höflich, P. 1995, ApJ, 443, 89
Höflich, P., & Khokhlov, A. M. 1996, ApJ, 457, 500
Hubble, E. 1936, ApJ, 84, 517
Hubble, E., & Tolman, R. C. 1935, ApJ, 82, 302
James, F., & Roos, M. 1994, MINUIT Function Minimization and Error Analysis (CERN Program Libr. Long Writeup D506; Geneva: CERN)
Kim, A., Goobar, A., & Perlmutter, S. 1996, PASP, 108, 190
La Violette, P. A. 1986, ApJ, 301, 544
Lee, A., Bloom E. D., & Petrosian V. 2000, ApJS, 131, 21
Leibundgut, B. 1988, Ph.D. thesis, Univ. Basel
Leibundgut, B., Tammann, G. A., Cadonau, R., & Cerrito, D. 1991, A&AS, 89, 537
Leibundgut, B., et al. 1996, ApJ, 466, L21
Lentz, E. J., Baron, E., Branch, D., Hauschildt, P. H., & Nugent, P. E. 2000, ApJ, 530, 966
Lira, P., et al. 1998, AJ, 115, 234
Marič, Z., Moles, M., & Vigier, J. P. 1977, Nuovo Cimento Lett., 18, 269
Metzger, M. R., et al. 1997, Nature, 387, 879
Narlikar, J. V. 1977, Ann. Phys., 107, 325
Narlikar, J. V., & Arp, H. C. 1993, ApJ, 405, 51
———. 1997, ApJ, 482, L119
Norris J. P., et al. 1995, ApJ, 439, 542
Nugent, P. 1997, Ph.D. thesis, Univ. Oklahoma, Chap. 4
Nugent, P., Baron E., Branch D., Fisher A., & Hauschildt P. 1997, ApJ, 485, 812
Nugent, P., Kim, A. G., & Perlmutter, S. 2001, PASP, submitted
Perlmutter, S., et al. 1997a, in Thermonuclear Supernova, ed. P. Ruiz-Lapuente, R. Canal, & J. Isern (Dordrecht: Kluwer), 749
———. 1997b, ApJ, 483, 565
———. 1999, ApJ, 517, 565
Phillips, M. M. 1993, ApJ, 413, L105
Pinto, P. A., & Eastman, R. G. 2000, ApJ, 530, 744
Piran, T. 1992, ApJ, 389, L45
Pskovskii, Y. P. 1977, Soviet Astron., 21, 675
———. 1984, Soviet Astron., 28, 658
Riess, A. G., Press, W. H., & Kirshner, R. P. 1995, ApJ, 438, L17
———. 1996, ApJ, 473, 88
Riess, A., et al. 1997a, AJ, 114, 722
———. 1998, AJ, 116, 1009
———. 1999a, AJ, 117, 707
———. 1999b, AJ, 118, 2675
———. 1999c, AJ, 118, 2668
Rust, B. W. 1974, Ph.D. thesis, Univ. Illinois (ORNL Rep. 4953)
Sandage, A., & Perelmutter, J. M. 1991, ApJ, 370, 455
Suntzeff, N. B., et al. 1999, AJ, 117, 1175
Weinberg, S. 1972, Gravitation and Cosmology: Principles and Applications of the General Theory of Relativity (New York: Wiley), 30
Wilson, O. C. 1939, ApJ, 90, 634
Zwicky, F. 1929, Proc. Nat. Acad. Sci., 15, 773